JOURNAL OF SOLID STATE CHEMISTRY 36, 45–51 (1981)

Crystal Structure and Charge Carrier Concentration of $W_{18}O_{49}$

K. VISWANATHAN AND K. BRANDT

Mineralogische–Petrographisches Institut, Braunschweig, West Germany

AND E. SALJE*

Mineralogisches Institut, Hannover, West Germany

Received November 28, 1979; in revised form March 26, 1980

The electrical resistivity of the tungsten oxide, $W_{18}O_{49}$, is $1.75 \cdot 10^{-3}$ Ω cm along the needle axis. The charge carrier density, as determined by reflectivity measurements, is $1.87 \cdot 10^{22}$ cm^{-3}, thereby indicating that most of the charge carriers are delocalized. Hence the smaller conductivity along the needle axis than that expected for such charge carrier concentrations must be found in the structure, which has been refined using the data collected with an automatic diffractometer. The structure consists of WO_6 and WO_7 polyhedra which are linked along edges and/or corners. However, as the linkage parallel to *b* takes place only by sharing corners, an anisotropy in the electrical conductivity may be expected. Another explanation for the smaller conductivity may be found in the occurrence of defects such as tunnels in the structure, which may scatter the electrons. The refinement shows that the tungsten positions, determined by Magneli (*Arkiv Kemi* **1**, 223 (1950)), are essentially correct; but the positions of the oxygens, especially two of them, differ considerably. This results in one of the tungsten atoms getting an additional coordinating oxygen, the coordination number thereby becoming seven.

Introduction

It is known since several years that if tungsten trioxide is reduced, different phases of nonstoichiometric composition appear. The change in the stoichiometry is effected by the formation of different types of defect structures. If the degree of reduction is such that the ratio O : W is larger than or equal to 2.82, then structures with "crystallographic shear planes" of corner-sharing octahedra occur (*1*). On the other hand, at higher degrees of reduction besides the phase $WO_{2.82}$, another one with composition, $WO_{2.72}$, appears. A preliminary analysis of $WO_{2.72}$ was carried out by Magneli (*2*), who observed that its structure contains distorted octahedra, linked together by sharing corners in such a way that extended tunnels are formed parallel to one of the three crystallographic axes. Magneli determined the tungsten positions with Patterson projections and estimated the positions of the oxygen atoms on the basis of packing considerations. The structure has been refined with the data obtained

* Author to whom correspondence should be addressed.

0022-4596/81/010045-07$02.00/0

using an automatic four-circle diffractometer, and the new atomic parameters are presented in this paper.

A striking feature of all reduced tungsten oxide phases is their valency distribution. Salje, Carley, and Roberts (*3*) found by means of ESCA experiments that pentavalent and hexavalent tungsten occur in all crystalline material. Accordingly, the formal valency distribution of $WO_{2.72}$ is $W_8^{6+}W_{10}^{5+}O_{49}$. The question arises whether these five valent states are fully localized and consequently two types of tungsten positions can be found in the structure, or whether the surplus electrons are mostly free under the formation of polaronic states (Berak and Sienko (*4*), Salje (*5*), Schirmer and Salje (*6*)). Hence, optical and electrical experiments were carried out to decide, whether the charge carriers are localized or not. The results are presented in this paper.

Crystal Preparation and Physical Properties

Crystals of $WO_{2.72}$ have been prepared by heating an appropriate mixture of WO_3 and W in evacuated, sealed silica tubes at 950°C. The product consisted of small plates and needles. A study under the microscope revealed that most plates are oriented intergrowths of several needle-shaped crystals. Their color is metallic red to purple. The individual needles are very fragile and can easily be bent.

The electrical conductivity was measured along the needle axis, which is parallel to the *b* axis. The crystal was glued between electrodes with silver paste and the a.c. resistivity was measured with a Wayne–Kerr Universal bridge (B642). No four-point measurements could be made because the crystals were too small and fragile. Instead, many two-point measurements were carried out on crystals of different sizes. Subsequently the effect of contact resistivity was eliminated by comparing the results obtained with crystals of different lengths but similar diameters. At room temperature, the specific resistivity has been determined to be 2.75 10^{-3} Ω cm. This value indicates a metallic conductivity of the same order of magnitude as that of $Na_{0.15}WO_3$ (*7*). The temperature dependence of the conductivity is given in Fig. 1.

The metallic behavior of $WO_{2.72}$ was also found in optical experiments. As the crystals were too small for single-crystal work, only reflection measurements were performed (*8*). The reflectivity of coarse-grained material, which is similar to the single crystal reflectivity (*9*), indicates the influence of quasi-free carrier reflection of the Drude type. The theoretical reflectivity (R) (Fig. 2) has been calculated using the formula

$$R \approx \left(\frac{\epsilon'^2 - 1}{\epsilon'^2 + 1}\right)^2,$$

with the (effective) real part of the dielectric constant $\epsilon' \approx \epsilon\left(1 - \omega_p^2 \Big/ \left(\frac{1}{\tau^2} + \omega^2\right)\right)$, in which ϵ is the dielectric constant of the background ions ($\epsilon \approx n^2$) and τ the dielectric relaxation time. The minimum reflectivity is then at ω_0 with

$$\omega_0 = \omega_p\left(\frac{\epsilon}{\epsilon - 1}\right)^{1/2}$$

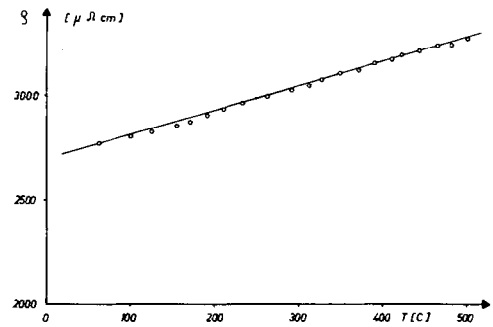

FIG. 1. Variation of resistivity of $W_{18}O_{49}$ with temperature.

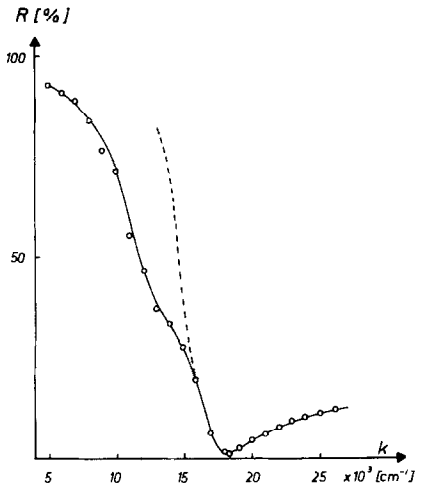

FIG. 2. Reflectivity vs wave number for $W_{18}O_{49}$. The dotted line represents the theoretical reflectivity calculated according to the Drude theory.

and $\epsilon = n^2 = 6.022$, the plasma frequency ω_p being $3.15 \cdot 10^{15}$ Hz (= 2.07 eV). The fitted relaxation time in Fig. 2 is $0.129 \cdot 10^{-14}$ sec. The correlated classical charge carrier density is $1.87 \cdot 10^{22}$ cm^{-3}, which is in good agreement with the hypothetical charge carrier density as determined from the nominal chemical composition ($n = 1.1 \cdot 10^{22}$ cm^{-3}). We, therefore, conclude that nearly all charge carriers are widely delocalized and should contribute to the conductivity. Nevertheless, the measured specific resistivity is much higher than expected (ca. $3 \cdot 10^{-5}$ Ω cm) for this carrier concentration and for a mobility similar to those of WO_3 (*4*) or sodium tungsten bronzes (*10*). Two different explanations of this discrepancy seem possible. First, the specific conductivity may be anisotropic with a smaller conductivity along *b*, the needle axis. As the conductivity cannot be measured in other directions because of the acicular habit of the crystals, this assumption cannot be verified experimentally. Nevertheless, the predominant linking of the tungsten octahedra along their edges in the plane perpendicular to *b* is likely to cause a greater conductivity parallel to the (010) plane. The second possibility is that the mobility may be drastically reduced by additional scattering of the electrons on the structural defects such as the tunnels. Which of these is likely is discussed later.

Crystal Structure Analysis

As all crystals were invariably twinned with $(20\bar{1})$ as twinning plane, the structure analysis had to be carried out using one such twinned crystal. As mentioned earlier, the needle-shaped crystals show the tendency to cluster together in parallel orientation to form approximately platy crystals, the cross section perpendicular to the plate being more eliptical than rectangular. The intensity data were collected using a four-circle Stoe automatic diffractometer and Mo$K\alpha$ radiation. In all, 3867 reflections were measured in the 2θ range from 0 to 50° and were reduced to 1825 independent reflections. Taking into consideration the relative orientation of the lattices of both the individuals of the twin and the width of the aperture at the detector, the reflections could be divided into three groups:

(1) reflections with intensities unaffected by overlap of both reciprocal lattices;

(2) those whose intensities are likely to be affected by partial overlap; and

(3) those which overlap exactly.

In doubtful cases the respective reflections were monitored on a strip chart during the measurement.

Only 1202 reflections, which belonged to groups (1) and (3), were considered for refinement and were duly given different scale factors. Atomic scattering factors for neutral atoms were taken from the International Tables (*11*) and anomalous scattering factors from Cromer and Libermann (*12*). The intensities were subjected to the usual polarization and absorption corrections. However, the absorption corrections are not likely to be very accurate because, for reasons mentioned earlier, the shape of the

crystal could not be described exactly. The crystal structure was determined using a slightly modified version of the ORFLS program. Only unit weights were used throughout. The tungsten positions of Magneli served as starting parameters and after four circles of refinement the R values came down to about 10%. Then a difference Fourier analysis was calculated to find the positions of the oxygen atoms. Further refinement including the oxygen positions and isotropic temperature factors brought the R value down to 6.5%. The refinement was stopped at this stage because the temperature factors of two tungsten atoms (W_1 and W_5) and three positions (O_{10}, O_{11}, O_{12}) started to become negative. This effect is probably due to the possible inaccuracy in the determination of the absorption correction referred to earlier. It was thought that reflections with 2θ values larger than 50° may give better temperature factors. However, as already pointed out by Magneli, there is a rapid decrease of intensity of reflections with increasing k index. A preliminary examination revealed that such reflections are too weak to influence the refinement considerably. Hence no further attempt was made to refine further with the available data.

The atomic coordinates are given in Table I, and the structure is shown in Fig. 3. The lattice constants, obtained with a Guinier camera are

$a = 18.334$ Å,
$b = 3.786$ Å,
$c = 14.044$ Å,
$\beta = 115.20°$ (space group $P2/m$).

The tungsten positions obtained in this investigation agree well with those found by Magneli. Discrepancies are, however, observed in the positions of the oxygen atoms. In particular, O_{22} and O_{24} differ by as much as 0.03–0.04 in their respective x parameters. This should not be surprising,

TABLE I

ATOMIC PARAMETERS

Atom	x	y	z
W(1)	0.0729	0.5	0.0017
W(2)	0.0863	0.5	0.2867
W(3)	0.1270	0.5	0.7589
W(4)	0.2214	0.5	0.5731
W(5)	0.2559	0.5	0.0098
W(6)	0.2759	0.5	0.2519
W(7)	0.3582	0.5	0.8640
W(8)	0.4141	0.5	0.5378
W(9)	0.4529	0.5	0.1681
O(1)	0.0792	0.0	0.0039
O(2)	0.0849	0.0	0.2803
O(3)	0.1305	0.0	0.7654
O(4)	0.2170	0.0	0.5784
O(5)	0.2590	0.0	0.0144
O(6)	0.2773	0.0	0.2453
O(7)	0.3620	0.0	0.8761
O(8)	0.4100	0.0	0.5405
O(9)	0.4501	0.0	0.1658
O(10)	0.0240	0.5	0.7258
O(11)	0.0373	0.5	0.1160
O(12)	0.1267	0.5	0.9112
O(13)	0.1334	0.5	0.4293
O(14)	0.1400	0.5	0.6450
O(15)	0.1825	0.5	0.1014
O(16)	0.1870	0.5	0.2830
O(17)	0.2470	0.5	0.8681
O(18)	0.2870	0.5	0.7100
O(19)	0.3111	0.5	0.5530
O(20)	0.3430	0.5	0.1530
O(21)	0.3584	0.5	0.3870
O(22)	0.3550	0.5	0.0100
O(23)	0.4400	0.5	0.8450
O(24)	0.5250	0.5	0.3150
O(25)	0.5	0.5	0.5

Note: Standard errors in tungsten parameters ±0.0001 and in oxygen parameters about ±0.0003.

as Magneli determined the oxygen parameters only on the basis of packing considerations. The tungsten position W_5 gets an additional coordinating oxygen at a distance of 1.812 Å (Table II.) (According to Magneli's parameters this O–O bond should be 2.616). The coordination number is thus seven instead of six. Surprisingly, the coordination polyhedra of W_5

TABLE II

IMPORTANT INTERATOMIC DISTANCES (Å)

Coordination around W(1)

W(1)–O distances		O–O distances		W(1)–W distances	
W(1)–O(1)	1.900	O(1)–O(11)	2.772	W(1)–W(1)[b]	2.648
–O(1)[a]	1.900	O(1)–O(11)[a]	2.814	–W(2)	3.894
–O(11)	1.971	O(1)–O(12)	2.648	–W(3)	3.932
–O(11)[b]	1.990	O(1)–O(15)	2.616	–W(2)[b]	3.845
–O(12)	1.910	O(11)–O(11)[a]	2.946	–W(5)	3.301
–O(15)	1.895	O(11)–O(15)	2.748	–W(6)	3.876
		O(11)–O(12)	2.859		
		O(12)–O(15)	2.420		

Coordination around W(5)

W(5)–O distances		O–O distances		W(5)–distances	
W(5)–O(5)	1.898	O(5)–O(12)	2.928	W(5)–W(1)	3.301
–O(5)[a]	1.898	O(5)–O(15)	2.917	–W(3)	3.301
–O(12)	2.172	O(5)–O(17)	2.735	–W(6)	3.260
–O(15)	2.221	O(5)–O(20)	2.684	–W(7)	3.308
–O(17)	1.925	O(5)–O(22)	2.604	–W(9)	3.333
–O(22)	1.812	O(12)–O(15)	2.420		
–O(20)	1.963	O(12)–O(17)	2.518		
		O(15)–O(20)	2.709		
		O(17)–O(22)	2.126		
		O(20)–O(22)	2.110		

[a] Atoms related by mirror plane.

[b] Atoms related by inversion center.

contains two very short oxygen–oxygen distances (O_{17}–O_{22} and O_{20}–O_{22}) although all other atomic distances (Table II) are well within the ranges of known O–O distances.

The structure is characterised by two features (Figs. 3 and 4): (1) The coordination of W_5 atoms by five other tungsten atoms in the plane ($O_{\frac{1}{2}}O$)in the form of a regular pentagon. (2) The nearly regular hexagonal vacant tunnels formed by the oxygens. The pentagons formed by tungsten are linked parallel to *b* by octahedra sharing corners, thereby forming pentagonal columns which run parallel to the hexagonal tunnels. Thus the structure can be described as consisting of pentagonal columns linked together laterally by zig-zag chains of W octahedra. These columns probably determine the needle shape of the crystals.

In order to estimate the type of bonding that mainly determines the structure the distances between the tungsten atoms of edge-sharing octahedra are compared with the lengths of the corresponding shared edges (Table III). It is observed that the smaller the lengths of the shared edge the greater is the distance between the corresponding tungsten atoms. It is well known that if edges of octahedra containing metal atoms with high valencies are shared and if the bond is predominantly ionic, then either the shared edges become short or the

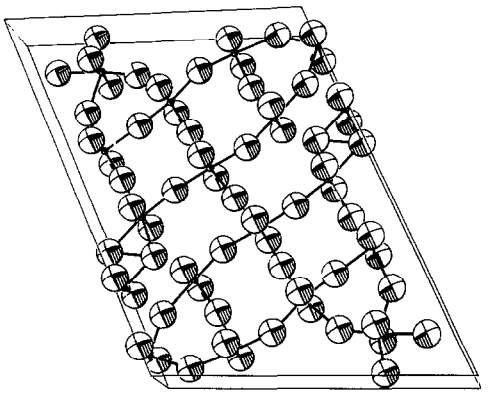

FIG. 3. Structure of $W_{18}O_{49}$, slightly tilted and viewed along *b*.

metal–metal distances tend to become larger or both. Such effects are attributed to the mutual repulsion between the adjoining metal ions. Hence if two metal ions of the same kind share edges an approximately direct relationship should be expected between the lengths of the shared edges, which are responsible for "screening" the repulsion and the metal–metal distances which are directly proportional to the repulsive forces. Hence a similar relationship should be expected between the two parameters if the forces between the W–W atoms are predominantly ionic. However, Table III indicates an inverse relationship which suggests that the forces are mainly covalent. It means that the structure must be interpreted as one, made up of linked

TABLE III

VARIATION OF W–W DISTANCES WITH THE LENGTHS OF THE SHARED EDGES

Lable	Distance between tungsten atoms (Å)	Length of the shared edges (Å)
W_1–W_1	2.648	2.946
W_5–W_6	3.260	2.709
W_5–W_3	3.301	2.518
W_5–W_7	3.308	2.126
W_5–W_9	3.333	2.110

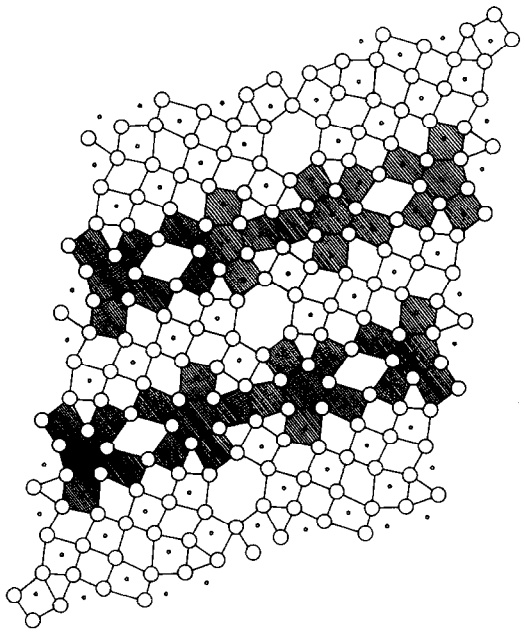

FIG. 4. A section $(x\frac{1}{2}z)$ in the structure of $W_{18}O_{49}$ showing the pentagonal columns of edge-shared WO_6 octahedra and hexagonal empty channels.

polyhedra rather than as one of closely packed oxygen atoms with tungsten atoms filling the gaps. The presence of spacious vacant channels appear to confirm the hypothesis. This is also in agreement with earlier results (*13*).

From the optical reflectivity and specific conductivity of $WO_{2.72}$ we know that the charge carriers are widely delocalized. It is interesting to find out, whether potential fluctuations due to inequivalencies of the different tungsten positions are likely in this structure. An examination of the structure reveals two types of clustering of W atoms, one along the *a* axis linked together as a continuous chain and the other containing the atoms W_2, W_4, and W_8, lying between such chains (Fig. 4). The former occupy octahedra which share at least one edge, whereas the latter share only corners with neighbouring octahedra. If we expect that the first set contains preferentially the W^{5+} states and the second set the W^{6+} positions

this would lead to a stronger overlap of $W^{5+}(d_{x^2-y^2})$ wavefunctions in the conducting bands along the *a* axis. Then the conduction band itself would have mainly a one dimensional character and consequently a considerable anisotropy can be expected in the specific conductivity. This would mean that the linkage of the polyhedra along the *b* axes is similar to WO_3 and hence a similar electronic mobility should be expected. However, the experimentally determined mobility is much lower in $WO_{2.72}$ than that in WO_3, which cannot be explained from an one dimensional overlap of W^{5+} wavefunctions. Moreover, the W–O distances in both sets of polyhedra are not so different as to suggest a segregation of W^{5+} and W^{6+} states.

The other alternative, which we prefer to explain the discrepancy in the conductivity involves a consideration of the electron-lattice interaction. Optical absorption of $WO_{2.72}$ and related compounds (*8*) show that—in contrast to metallic Na_xWO_3 ($x > 0.25$)—charge carriers behave like polarons with considerable electron–phonon coupling. In ESCA spectra the W^{5+} level is shifted by 1.2 eV with respect to W^{6+} and no final state effects similar to tungsten bronzes (*14*) have been observed. We, therefore, think that $WO_{2.72}$ shows polaronic conductivity like WO_3 and H_xWO_3 ($x \ll 0.1$) (*6, 8*), which is extremely sensitive to inequivalencies of lattice sites and scattering at structural defects. Both effects reduce the mobility. In $WO_{2.72}$ inequivalent tungsten positions occur in and between the chains. In addition, defects such as tunnels are also present (Fig. 4). Hence we believe that the reduced mobility is mainly to such structural imperfections and not due to the localization of electrons by W^{5+} atoms occupying fixed positions.

Finally, a look at the projection (*h*01) explains why $WO_{2.72}$ tends to develop twins. The trace of the plane ($\bar{2}01$) goes through the W_5 atoms which are related by the inversion center, thereby dividing the coordination polyhedron, the pentagon, into two similar halves. As the structure near this line is extremely similar on both sides, the energy required for the formation of a twin along ($\bar{2}01$) must be very low and therefore the probability to find twinned crystals is very high.

Acknowledgment

We are indebted to the Deutsche Forschungsgemeinschaft, West Germany, for financial support.

References

1. R. Pickering and R. J. D. Tilley, *J. Solid State Chem.* **16,** 247 (1976).
2. A. Magneli, *Arkiv Kemi* **1,** 223 (1950).
3. E. Salje, A. F. Carley, and M. W. Roberts, *J. Solid State Chem.* **29,** 237 (1979).
4. J. M. Berak and M. J. Sienko, *J. Solid State Chem.* **2,** 109 (1970).
5. E. Salje, *Opt. Commun.* **24,** 231 (1978).
6. O. W. Schirmer and E. Salje, *Solid State Comm.*, in press.
7. P. A. Lightsey, S. A. Lilienfeld, and D. F. Holcomb, *Phys. Rev. B* **14,** 4730 (1976).
8. E. Salje and G. Hoppmann, *Philos. Mag.*, in press.
9. P. G. Dickens, R. M. P. Quilliam, and M. S. Whittingham, *Mat. Res. Bull.* **3,** 941 (1968).
10. N. F. Mott, *Philos. Mag.* **35,** 111 (1977).
11. "International Tables of Crystallography," Kynoch Press (1952).
12. D. T. Cromer and D. Libermann, *J. Chem. Phys.* **53,** 1891 (1970).
13. E. Salje, *Acta Cryst. Sect. A* **32,** 233 (1976).
14. G. K. Wertheim, *Chem. Phys. Lett.* **65,** 377 (1979).